frontiers in Materials

ORIGINAL RESEARCH
published: 10 June 2020
doi: 10.3389/fmats.2020.00149

Effect of Titanium on Microstructure, Texture, and Mechanical Property of As-Extruded Mg—Sn Alloy

Zhengwen Yu[1,2], *Chang Zhang*[1], *Aitao Tang*[2], *Caiyu Li*[1], *Jianguo Liu*[1], *Zhengyuan Gao*[3]* *and Fusheng Pan*[2]

[1] Key Laboratory of Oral Disease Research, School of Stomatology, Zunyi Medical University, Zunyi, China, [2] College of Materials Science and Engineering, Chongqing University, Chongqing, China, [3] School of Mechatronics and Vehicle Engineering, Chongqing Jiaotong University, Chongqing, China

The effect of titanium on the microstructure, the texture, and the mechanical properties of as-extruded Mg–Sn alloy has been investigated in the present work. The result reveals that the alloy subjected to the optimized extrusion process shows an extremely refined microstructure with an average grain size of 1.7 μm. Meanwhile, the addition of titanium has an obvious effect on intensifying the basal texture where the basal slip cannot be easily activated during tensile testing. As a result, the alloy shows excellent mechanical properties where yield strength and elongation are 200 MPa and 30.2%, respectively. The enhanced yield strength of the alloy can be attributed to the extremely refined microstructure and the intensified basal texture, while the improved elongation of the alloy can be explained by the ultra-fine-grained microstructure through reducing the critical resolved shear stress that favors the prismatic slip activity to accommodate the basal slip.

Keywords: magnesium alloy, microstructure, TEM, mechanical properties, orthopedic implant

OPEN ACCESS

Edited by:
Lai-Chang Zhang,
Edith Cowan University, Australia

Reviewed by:
Jiejun He,
Guizhou Institute of Technology, China
Bo Song,
Southwest University, China
Daokui Xu,
Institute of Metals Research (CAS), China

***Correspondence:**
Zhengyuan Gao
zhengyuangao@cqjtu.edu.cn

Specialty section:
This article was submitted to Structural Materials, a section of the journal Frontiers in Materials

Received: *26 March 2020*
Accepted: *28 April 2020*
Published: *10 June 2020*

Citation:
Yu Z, Zhang C, Tang A, Li C, Liu J, Gao Z and Pan F (2020) Effect of Titanium on Microstructure, Texture, and Mechanical Property of As-Extruded Mg—Sn Alloy. Front. Mater. 7:149. doi: 10.3389/fmats.2020.00149

INTRODUCTION

Metallic biomaterials, such as stainless steel, titanium alloys, cobalt-based alloys, zirconium alloys, and nitinol shape memory alloy, are widely applied as orthopedic implants and cardiovascular stents to heal or replace the damaged bones and vessels (Bahl et al., 2018; Bekmurzayeva et al., 2018; Mehjabeen et al., 2018; Hernandez-Rodriguez et al., 2019; Kaur and Singh, 2019; Takale and Chougule, 2019). However, the elastic moduli of these metallic implants are significantly higher than that of the human natural bone, leading to a stress shielding effect (Majumdar et al., 2018). The harmful metallic ions released from the implants because of the degradation of the implants inside the organism, as well as the debris due to wear, could result in inflammation in the vicinity of the implants (Noronha Oliveira et al., 2018; Costa et al., 2019). Therefore, seeking a novel metallic implant with excellent biocompatibility and mechanical properties, with the elastic moduli close to that of the natural bone, and outstanding degradable properties has become one of the current frontiers in metallic biomaterials.

Magnesium and its alloys have attracted a great attention in the fields of medical devices and orthopedic implants because of their relatively low density (1.74 g/cm^3) which is very close to that of the human bone (1.8–2.1 g/cm^3), excellent biocompatibility, and favorable biodegradability in human physiological conditions (Haghshenas, 2017; Bian et al., 2018; Cui et al., 2018; Gu et al., 2018; Jiang et al., 2018; Bommala et al., 2019; Liu P. et al., 2019). Moreover, the elastic modulus of Mg alloys (40–45 GPa) is much closer to that of the human natural bone (10–30 GPa) compared

with stainless steel (193 GPa), titanium and its alloys (110–117 GPa), cobalt-based alloys (200 GPa), and nitinol shape memory alloy (24–83 MPa) (Lv et al., 2018; Salleh et al., 2018; Song et al., 2018; Ban et al., 2019; Li et al., 2019). However, the major challenges for magnesium and its alloys are insufficient mechanical properties, high biodegradation rate in physiological environments, poor corrosion fatigue, and stress corrosion cracking (Wang et al., 2019a,b,c,d,e). As a result, the rapid degradation rate of the implants could lead to the loss of mechanical integrity before healing. The accumulation of metallic ions and a high rate of hydrogen evolution could also increase the local pH value, thus deteriorating the surrounding tissue (Li et al., 2018). Therefore, the mechanical properties and the corrosion resistance of Mg alloys can be effectively improved through the addition of alloying elements. Various kinds of Mg alloys, such as Mg–Al based alloys, Mg–Zn-based alloys, Mg–Li-based alloys, Mg–Sr-based alloys, Mg–Ca-based alloys, and Mg–Sn-based alloys, have been investigated to determine their effectiveness as orthopedic implants or cardiovascular stents (He et al., 2015; Hou et al., 2016; Li et al., 2016; Liu et al., 2017; Zhao et al., 2017; Bian et al., 2018; Jiang et al., 2018, 2019).

The selection of alloying elements used in the human body without a harmful effect is limited, according to previous investigations. Sn is the most important candidate applied as alloying element in magnesium biomaterials because Sn is one of the nutrient elements found in the human body, and the daily intake of Sn in the human body is 1–3 mg (Liu Y. et al., 2019). In addition, Sn has an obvious effect on promoting the synthesis of nucleic acids and proteins (Chen et al., 2014; Radha and Sreekanth, 2017). According to previous investigations, the Mg−1Sn alloy extract with Sn concentration of 15.8 ± 7.8 μM/L did not induce cell cytotoxicity except for ECV304. Additionally, the released metallic ions of Sn^{4+} did not induce cytotoxicity in both L-929 and MC3T3-E1 cells even at high concentrations of 66.5 and 1.11 mM/L, respectively. As a result, the Mg–Sn alloy exhibits good biocompatibility, although the released metallic ions of Sn^{2+} in Mg–Sn-based alloy extracts at rather low concentrations of 0.141 and 0.025 mM/L could induce severe cytotoxicity in L-929 and MC3T3-E1 cells, respectively (Yamamoto et al., 1998; Gu et al., 2009; Kubásek et al., 2013). However, the mechanical properties of Mg–Sn-based alloys are lower than those of WE43 magnesium alloy applied as orthopedic implant (Zhen et al., 2014). The main reason could be attributed to the rod-like precipitation morphology of the Mg_2Sn phase lying on the basal planes, showing poor precipitation hardening behavior [26]. Therefore, investigations have been initiated to improve the mechanical properties of Mg–Sn-based alloys through alloying elements (Pan et al., 2015; She et al., 2015; Pan F. et al., 2016; Pan H. et al., 2016; Peng et al., 2018, 2019; Liao et al., 2019; Song et al., 2019; Wang et al., 2019f).

Titanium and its alloys are the most important metallic medical devices applied as orthopedic implants because of their outstanding biocompatibility, excellent mechanical properties, and good corrosion resistance *in vivo*. However, Ti is seldom applied in magnesium and its alloys because of its extremely high melting temperature compared with magnesium and its limited solid solubility in Mg. Our previous work figured out that the addition of titanium in AZ91 magnesium alloy could effectively refine the microstructure and improve the mechanical properties at room temperature (Yu et al., 2014). Other investigations also proved that the addition of titanium could tailor the microstructure and improve the mechanical properties and corrosion resistance (Candan et al., 2016; Koltygin et al., 2017; Yu et al., 2017). Therefore, the addition of titanium in as-extruded Mg−1Sn alloy has been investigated in the present work, aiming at elucidating the effect of titanium on the microstructure, the texture, and the mechanical properties of as-extruded Mg–Sn alloy at room temperature.

TABLE 1 | Chemical compositions of as-extruded alloys (wt.%).

Alloy	Sn	Ti	Others	Mg
Mg-1Sn	1.06	-	< 0.01	Bal.
Mg-1Sn-0.1Ti	0.92	0.09	<0.01	Bal.

MATERIALS AND METHODS

Synthesis of Mg–Sn and Mg–Sn–Ti Alloys

Commercial pure Mg (99.98 wt.%), pure Sn (99.98 wt.%), and Sn−10Ti (wt.%) master alloy were applied as raw materials. Experimental alloys, named as Mg−1Sn and Mg−1Sn−0.1Ti alloys, were melted in a steel crucible inside an induction melting furnace under an argon atmosphere protection and then followed by water quenching. The ingots covered with graphite were homogenized at 500°C for 24 h and then followed with water quenching immediately. The skinned ingots were preheated to 250°C for 2 h and then extruded in an XJ-500 horizontal extruder. Solid rods, ∼16 mm in diameter and corresponding to an extrusion ratio of 25:1, were extruded at an extrusion rate of 20 mm s^{-1} and air-cooled (Yu et al., 2015).

Characterization of As-extruded Mg–Sn and Mg–Sn–Ti Alloys

The rectangular specimens for microstructure characterization were machined from as-extruded rods and ground using silicon carbide (SiC) paper up to 1,000 grit, followed by ultrasonic cleaning and drying by cold air.

The analyzed chemical compositions of as-extruded alloys, which were measured by inductively coupled plasma atomic emission spectrometry, are listed in **Table 1**. The phase constitution and the texture were determined by using X-ray diffraction (XRD; Rigaku D/MAX-2500PC). The measurements were performed on longitudinal sections of the specimens.

Orientation mapping was performed on the cross-sections of the extruded bars by using the electron backscatter diffraction (EBSD) technique in focused ion beam scanning electron microscopy. An accelerating voltage of 20 kV and a step size of 0.1 μm were used. The sample surfaces were prepared in the same way as for metallography and were then electrochemically polished in a commercial AC2 solution. A software HKL Chanel 5 System was utilized to process the data obtained from the

EBSD measurements. The indexing percentage in our experiment was 79%.

The transmission electron microscopy (TEM) foils of all the samples were prepared by twin-jet electro-polishing using a solution of 5.3 g LiCl, 11.6 g $Mg(ClO_4)_2$, 500 ml methanol, and 100 ml 2-butoxy-ethanol at ∼-50°C and 90 V. The specimens were surface-cleaned by ion milling using a Gatan Precision Ion Polishing System (PIPS) at an operating voltage of 2 kV.

Tests of the Mechanical Properties of As-extruded Mg–Sn and Mg–Sn–Ti Alloys

Tensile and compressive tests were carried out at room temperature by using a materials testing machine at a loading rate of 3 mm min^{-1} to determine the mechanical properties of as-extruded alloys. The samples for tensile (gauge length l_g = 25 mm, diameter Φ = 5 mm) and compression (l_g = 12 mm, diameter Φ = 8 mm) tests shown in **Figure 1** were machined parallel to the extrusion axis (Yu et al., 2015).

RESULTS

Phase Components

The XRD patterns and the texture along the extrusion direction (ED) of as-extruded alloys are shown in **Figure 2** in the present work. In **Figure 2A**, the phase constitution of as-extruded Mg−1Sn alloy is α-Mg matrix, while the XRD pattern of as-extruded Mg−1Sn−0.1Ti alloy shown in **Figure 2B** is also indexed as α-Mg matrix. According to previous investigations, Mg_2Sn precipitates cannot be indexed by XRD in Mg−1Sn alloy because of the relatively high solubility of Sn in α-Mg matrix, and secondary-phase α-Ti is hardly found in Mg alloys as well because of its extremely low solubility in Mg and relatively high melting point compared with Mg (Yu et al., 2014; She et al., 2016; Tong et al., 2017). That is the main reason why the phase components of both as-extruded Mg−1Sn and Mg−1Sn−0.1Ti alloys are α-Mg matrix in the present work.

Texture

The textures of the alloys in forms of (0002) and $(10\bar{1}0)$ pole figures along the ED in the present investigation are shown in **Figure 3**. Obviously, both of the alloys subjected to the extrusion process in the present work show a typical fiber texture, where the majority of the grains with their (0002) planes were parallel to the ED. In addition, the maximum value of texture intensity for as-extruded Mg−1Sn−0.1Ti alloy is about 4.8 in **Figure 3B**, which is nearly two times compared to that of as-extruded Mg−1Sn alloy shown in **Figure 3A**. Therefore, the basal slip of as-extruded Mg−1Sn−0.1Ti alloy, according to the previous investigation, cannot be prone to be activated when tension stress is loaded along the ED compared with Mg−1Sn alloy (He et al., 2013).

EBSD

To further understand the microstructure evolution of both as-extruded Mg−1Sn and Mg−1Sn−0.1Ti alloys in the present work, EBSD technique has been applied in the form of inverse pole figure, grain size distribution, and texture as shown in **Figure 4**. Note that the EBSD maps are taken from the cross-section (extrusion axis perpendicular to the sample plane) of the alloy. Obviously, there is a higher proportion of either blue-colored or green-colored grains in both as-extruded Mg−1Sn and as-extruded Mg−1Sn−0.1Ti alloys in **Figures 4a,d**. The grain size distributions of the alloys in the present work are shown in **Figures 4b,e**. In **Figure 4b**, the grain size of as-extruded Mg−1Sn alloy ranges from 1 to 17 μm, and the average grain size of the alloy is 9.6 μm. Meanwhile, the addition of titanium shows a significant grain refinement effect in the present work. In **Figure 4e**, the grain size distribution of as-extruded Mg−1Sn−0.1Ti alloy indicates that the majority of the grains are <3.0 μm, and the calculated average grain size of the alloy is 1.7 μm. Therefore, as-extruded Mg−1Sn−0.1Ti alloy shows an obvious grain size strengthening effect, leading to improved strength compared with as-extruded Mg−1Sn alloy. In addition, the textures of the specimens are also examined by EBSD technique, and the results are in accordance with the textures examined by XRD as shown in **Figure 3**.

TEM

The bright-field image of as-extruded Mg−1Sn−0.1Ti alloy in the present work is shown in **Figure 5**. As clearly seen from **Figure 5a**, there are irregular spheroid precipitates observed in the matrix of as-extruded Mg−1Sn−0.1Ti alloy. The energy dispersive x-ray spectroscopy result shown in **Figure 5c** demonstrates that the secondary phases have been identified as Mg_2Sn, although it has not been detected in the present work by the XRD shown in **Figure 2**. Moreover, none of the intermetallic compounds containing titanium was found, and the main reason can be attributed to the extremely low concentration of titanium. Selected area electron diffraction patterns of the matrix and the second phase have been indexed in **Figures 5d,e**, respectively. Previous investigations pointed out that the Mg_2Sn phase exhibited different morphologies and orientation relationship between the matrix and the precipitation under different heat treatment conditions (Zhang et al., 2008; Gibson et al., 2010). Moreover, investigations also illustrated that the morphology and the orientation relationship of the second phase had an obvious effect on enhancing the strength of magnesium alloys. According to their conclusions, prismatic precipitate plates showed a stronger precipitation hardening effect than the other precipitates, such as basal precipitate plates, [0001]α precipitate rods, spherical particles, and so on (Nie, 2003, 2012). In the present investigation, the morphology of Mg_2Sn precipitates has been identified as irregular spherical particles, and the orientation relationship between the matrix and the precipitation in this paper has been indexed as $(0001)_{Mg}$ // $(111)_{Mg_2Sn}$ and $< 11\bar{2}0 >_{Mg}$ // $< 1\bar{1}0 >_{Mg_2Sn}$.

Mechanical Properties

The typical nominal tensile and compressive stress—strain curves of both as-extruded Mg−1Sn and Mg−1Sn−0.1Ti alloys are shown in **Figure 6**, and the room temperature mechanical properties are listed in **Table 2**. Obviously, as-extruded Mg−1Sn−0.1Ti alloy, compared with as-extruded Mg−1Sn alloy, shows excellent mechanical properties at room

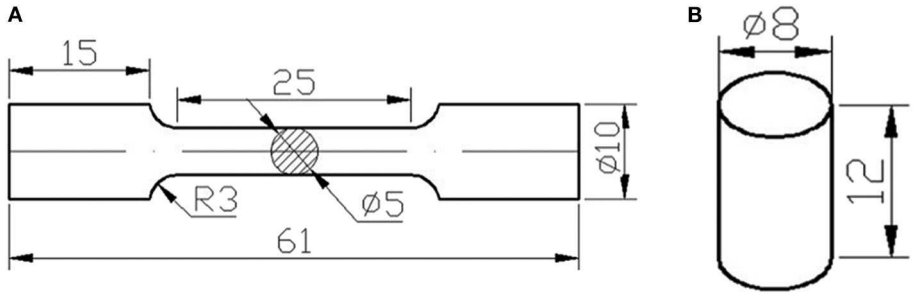

FIGURE 1 | Schematic diagrams of **(A)** tensile and **(B)** compressive samples machined from as-extruded profiles.

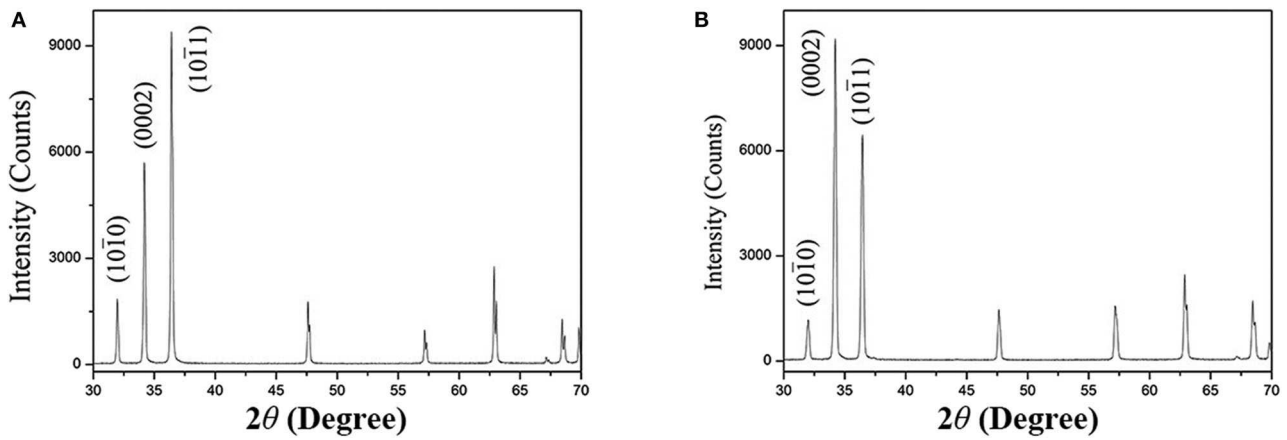

FIGURE 2 | X-ray diffraction patterns of **(A)** as-extruded Mg−1Sn alloys and **(B)** as-extruded Mg−1Sn−0.1Ti alloys.

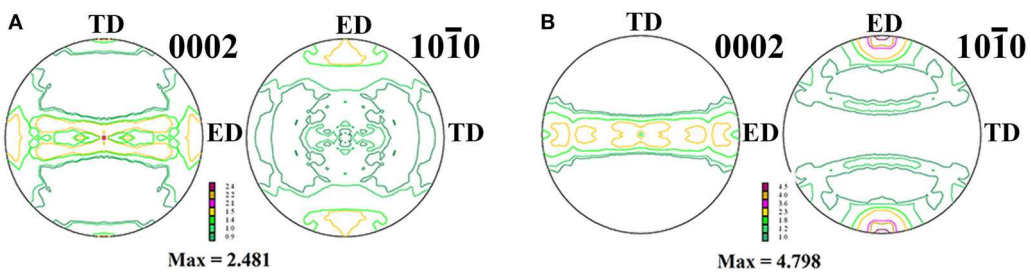

FIGURE 3 | Pole figures of **(A)** as-extruded Mg−1Sn alloys and **(B)** as-extruded Mg−1Sn−0.1Ti alloys. The maximum values of texture intensities are ∼2.48 and ∼4.80, respectively.

temperature. In the present investigation, as-extruded Mg−1Sn alloy shows a yield strength (YS) of 163 MPa, an ultimate tensile strength (UTS) of 231 MPa, and a tensile elongation to fracture (δ_T) of 18.3% at ambient temperature. Upon the addition of titanium into Mg−1Sn alloy, the YS, UTS, and δ_T of the alloy are 200 MPa, 230 MPa, and 30.2%, respectively. Compared with as-extruded Mg−1Sn alloy, the YS and δ_T of as-extruded Mg−1Sn−0.1Ti alloy have been improved to about 22.7 and 65%, respectively. More importantly, as-extruded Mg−1Sn−0.1Ti alloy, in terms of orthopedic implant, has favorable mechanical properties compared with WE43 magnesium alloy which feature YS of 190–220 MPa (200 MPa for Mg−1Sn−0.1Ti alloy) and δ_T of 20–35% (30.2% for Mg−1Sn−0.1Ti alloy) (Schaller et al., 2016).

DISCUSSION

In magnesium and its alloys, ultra-fine grained microstructure, intensified basal texture, solid solution additions, and precipitates have obvious effects on improving the mechanical properties of the alloys (Nie, 2003, 2012; Yu et al., 2015; Pan et al., 2018; Yu Z. et al., 2018). In addition, a previous investigation figured

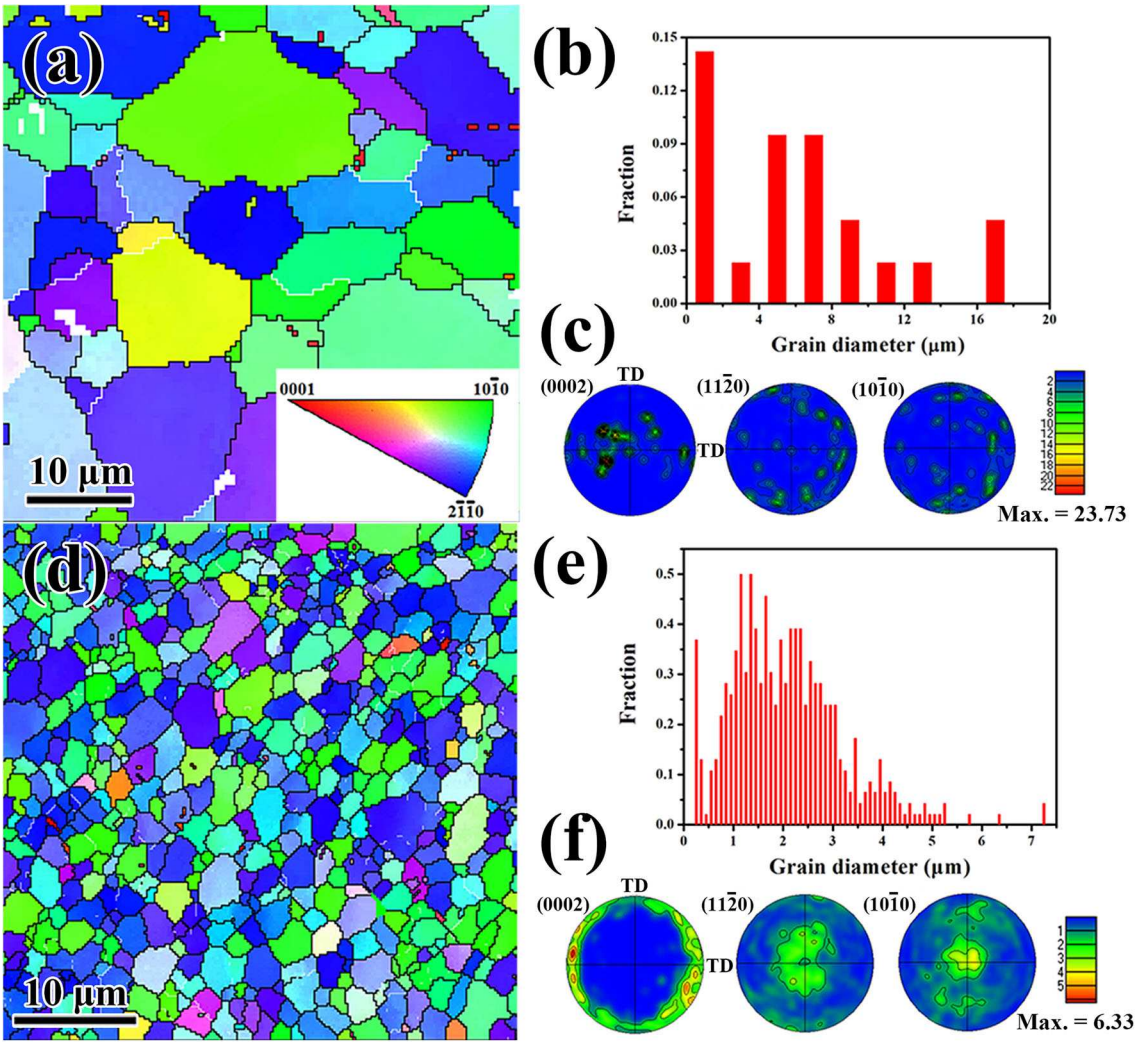

FIGURE 4 | Inverse pole figure maps of **(a)** as-extruded Mg−1Sn alloys and **(d)** as-extruded Mg−1Sn−0.1Ti alloys. Grain size distributions of **(b)** as-extruded Mg−1Sn alloys and **(e)** as-extruded Mg−1Sn−0.1Ti alloys. Textures of **(c)** as-extruded Mg−1Sn alloys and **(f)** as-extruded Mg−1Sn−0.1Ti alloys. The extruson axis is parallel to the image plane.

out that Ti could prevent the fusion of grain boundary (Zhang et al., 2015). As a result, as-extruded Mg−1Sn−0.1Ti alloy that was subjected to a low-temperature extrusion process shows an ultra-fine-grained microstructure. The extremely refined microstructure with an average grain size of ∼1.7 μm takes a significant effect on improving the strength according to the Hall–Petch relation (Yu H. et al., 2018). In addition, the ultra-fine-grained microstructure also plays an important part in improving the ductility of magnesium alloys at room temperature. According to previous investigations, extension twinning and prismatic slip are difficult to be activated due to their higher critical resolved shear stress (CRSS) than basal slip (He et al., 2013). However, our previous investigations proved that the ultra-fine-grained microstructure could effectively decrease the ratio of $CRSS_{prismatic}/CRSS_{basal}$, resulting in the activation of prismatic slip to accommodate basal slip (Yu et al., 2015; Yu Z. et al., 2018). Therefore, the ultra-fine grained microstructure of as-extruded Mg−1Sn−0.1Ti alloy, in the present work, can be considered as the dominant reason why as-extruded Mg−1Sn−0.1Ti alloy shows superior elongation at room temperature.

Usually, magnesium and its alloys subjected to the hot extrusion process show a typical fiber texture, where the majority of the grains in the alloy have their basal planes parallel to ED. In this case, the alloy shows an extremely low orientation factor, which is nearly 0 in theory (He et al., 2013). In other words, the activity of basal slip requires higher shear stress when tension load is applied along ED, leading to higher yield strength at room temperature. Plenty of investigations have also proven that the basal slips of the textured Mg alloys are limited when tension stress is applied parallel to the loading direction (He et al., 2013; Yu et al., 2015; She et al., 2016; Peng et al., 2018, 2019; Yu Z. et al.,

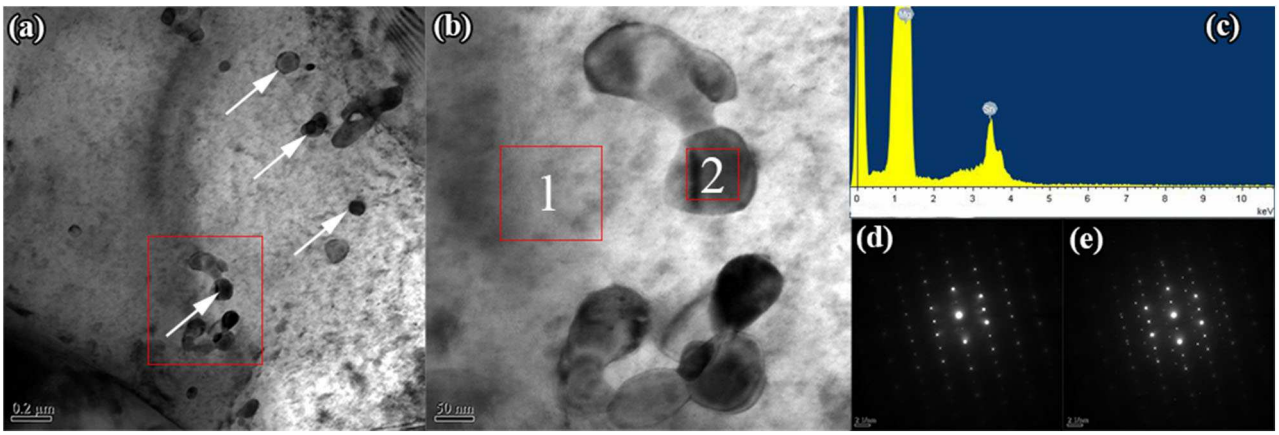

FIGURE 5 | Transmission electron microscopy image of as-extruded Mg−1Sn−0.1Ti alloy. **(a)** Bright-field image, **(b)** enlarged view of the red rectangle inset of **(a)**; **(c)** energy dispersive x-ray spectroscopy result of the precipitate inset of **(b)** marked 2, and **(d,e)** selected area electron diffraction patterns of the matrix and the precipitate marked 1 and 2 in **(b)**, respectively.

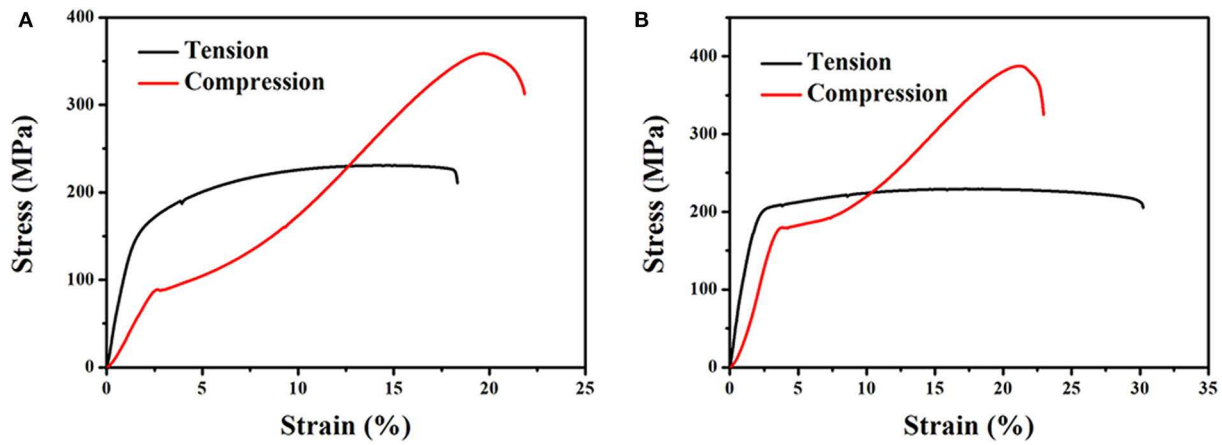

FIGURE 6 | Stress–strain curves of **(A)** as-extruded Mg−1Sn alloys and **(B)** as-extruded Mg−1Sn−0.1Ti alloys.

2018; Song et al., 2019). In the present work, Mg−1Sn−0.1Ti alloy subjected to the low temperature extrusion process shows a strong basal texture (**Figure 3B**). If the tension load applied along ED is applied on the specimen as investigated in this paper, the basal slip of the alloy is difficult to be activated compared with that of Mg−1Sn alloy. As a result, as-extruded Mg−1Sn−0.1Ti alloy shows superior yield strength than as-extruded Mg−1Sn alloy that was subjected to the same extrusion condition in the present investigation.

In addition, precipitates, including morphologies and the orientation relationship between the matrix and the precipitates, have an obvious effect on improving the mechanical properties of Mg alloys (Nie, 2003, 2012). Our previous investigations have proven that a great number of nano-scaled precipitates in the matrix show a strong pinning effect on dislocation motion, leading to the enhancement of strength during tension and compression parallel to ED (Yu et al., 2015; Yu Z. et al., 2018). Meanwhile, other investigations have also demonstrated that the morphologies and the orientation relationship can significantly affect the strength of Mg alloys (Nie, 2003, 2012). In the present work, there is a large number of fine, irregular, spheroidal Mg_2Sn precipitates as observed in **Figure 5**, and the orientation relationship between the α-Mg matrix and the Mg_2Sn precipitates has been indexed as $(0001)_{Mg}$ // $(111)_{Mg_2Sn}$ and $< 11\bar{2}0 >_{Mg}$ // $< 1\bar{1}0 >_{Mg_2Sn}$, which is observed elsewhere (She et al., 2016). As a result, the morphologies and the orientation relationship of the precipitates in the present work show a weaker effect than the other precipitates (e.g., plate-like intermetallic compounds precipitating along the *c*-axis). However, the nano-scaled precipitates take an obvious effect on improving the strength of the alloy through pinning the dislocation motion during stress application on the alloy.

In conclusion, Mg−1Sn−0.1Ti alloy, with the addition of nutritive elements, is suitable for orthopedic implant due to its good mechanical properties. The degradation behavior and the biocompatibility of the alloy will be discussed in our further work.

TABLE 2 | Mechanical properties of Mg-1Sn and Mg-1Sn-0.1Ti alloys.

Alloys	Tension			Compression		
	TYS	UTS	δ_T	CYS	UCS	δ_C
Mg-1Sn	163	231	18.3	89	358	21.8
Mg-1Sn-0.1Ti	200	230	30.2	180	387	22.9

CONCLUSIONS

The microstructure and the mechanical properties of as-extruded Mg−1Sn−0.1Ti alloy have been investigated in the present work. The major conclusions are summarized as follows:

- Mg−1Sn−0.1Ti alloy shows an ultra-fine-grained microstructure and an intensified basal texture.
- There is a large number of fine, irregular, spheroidal Mg_2Sn precipitates lying in the matrix. The orientation relationship between the α-Mg matrix and the Mg_2Sn precipitates has been indexed as (0001)Mg // (111)Mg_2Sn and $< 11\bar{2}0 >$Mg // $< 1\bar{1}0 >Mg_2Sn$.
- Mg−1Sn−0.1Ti alloy exhibits excellent mechanical properties, where yield strength and elongation are respectively 200 MPa and 30.2% at room temperature.
- The improved yield strength can be attributed to the ultra-fine-grained microstructure, intensified basal texture, and nano-scale, fine, spheroidal Mg_2Sn precipitates pinning the dislocation motion.
- The superior elongation property of as-extruded Mg−1Sn−0.1Ti alloy can be explained as an extremely fine microstructure by reducing the critical resolved shear stress that favors the prismatic slip activity, thus accommodating basal slip.

DATA AVAILABILITY STATEMENT

The raw data supporting the conclusions of this article will be made available by the authors, without undue reservation, to any qualified researcher.

AUTHOR CONTRIBUTIONS

ZG and ZY conceived and designed the study and experiment plan and wrote the paper. CZ performed the experiments. CZ and CL built FM model and do the numerical simulation. AT and JL analyzed the experiment result. AT, JL and FP reviewed and edited the manuscript. All authors read and approved the manuscript.

FUNDING

The present work is supported by National Natural Science Foundation of China (Project 51474043), the Scientific and Technological Research Program of Chongqing Municipal Education Commission (Grant No. KJQN201800731) and the Scientific and Technological Research Program of Chongqing Science and Technology Bureau (Grant No. cstc2019jcyj-msxmX0761), Organization Department of Guizhou Provincial Party Committee (RCJD2018-9), Guizhou Education Department Youth Science and Technology Talents Growth Project [KY (2016) 207], Opening Project of Guizhou Education Department Special Key Laboratory of Oral Disease Research (SKLODR201703), Joint Funds of Zunyi Science and Technology Bureau and Zunyi Medical University Hospital of Stomatology [ZYKHSZ (2018) 240], Joint Funds of Zunyi Science and Technology Bureau and Zunyi Medical University [ZYKHSZ (2017) 25], Ph.D. Starting Foundation of Zunyi Medical University (F-868) and Academic Talents and Innovation Program of Zunyi Medical University [QKHPTRC(2017)5733-057].

REFERENCES

Bahl, S., Aleti, B. T., Suwas, S., and Chatterjee, K. (2018). Surface nanostructuring of titanium imparts multifunctional properties for orthopedic and cardiovascular applications. *Mater. Des.* 144, 169–181. doi: 10.1016/j.matdes.2018.02.022

Ban, H., Bai, R., Yang, L., and Bai, Y. (2019). Mechanical properties of stainless-clad bimetallic steel at elevated temperatures. *J. Constr. Steel Res.* 162:105704. doi: 10.1016/j.jcsr.2019.105704

Bekmurzayeva, A., Duncanson, W. J., Azevedo, H. S., and Kanayeva, D. (2018). Surface modification of stainless steel for biomedical applications: revisiting a century-old material. *Mater. Sci. Eng. C* 93, 1073–1089. doi: 10.1016/j.msec.2018.08.049

Bian, D., Jiang, J., Zhou, W., Li, N., Zheng, Y., Leeflang, S., et al. (2018). *In vitro* characterization of ZM21 mini-tube used for biodegradable metallic stent. *Mater. Lett.* 211, 261–265. doi: 10.1016/j.matlet.2017.09.092

Bommala, V. K., Krishna, M. G., and Rao, C. T. (2019). Magnesium matrix composites for biomedical applications: a review. *J. Magn. Alloys* 7, 72–79. doi: 10.1016/j.jma.2018.11.001

Candan, S., Celik, M., and Candan, E. (2016). Effectiveness of Ti-micro alloying in relation to cooling rate on corrosion of AZ91 Mg alloy. *J. Alloys Compd.* 672, 197–203. doi: 10.1016/j.jallcom.2016.02.043

Chen, Y., Xu, Z., Smith, C., and Sankar, J. (2014). Recent advances on the development of magnesium alloys for biodegradable implants. *Acta Biomater.* 10, 4561–4573. doi: 10.1016/j.actbio.2014.07.005

Costa, B. C., Tokuhara, C. K., Rocha, L. A., Oliveira, R. C., Lisboa-Filho, P. N., and Costa Pessoa, J. (2019). Vanadium ionic species from degradation of Ti-6Al-4V metallic implants: *in vitro* cytotoxicity and speciation evaluation. *Mater. Sci. Eng. C* 96, 730–739. doi: 10.1016/j.msec.2018.11.090

Cui, L., Sun, L., Zeng, R., Zheng, Y., and Li, S. (2018). *In vitro* degradation and biocompatibility of Mg-Li-Ca alloys—the influence of Li content. *Sci. China Mater.* 61, 607–618. doi: 10.1007/s40843-017-9071-y

Gibson, M. A., Fang, X., Bettles, C. J., and Hutchinson, C. R. (2010). The effect of precipitate state on the creep resistance of Mg–Sn alloys. *Scr. Mater.* 63, 899–902. doi: 10.1016/j.scriptamat.2010.07.002

Gu, X., Wang, F., Xie, X., Zheng, M., Li, P., Zheng, Y., et al. (2018). *In vitro* and *in vivo* studies on as-extruded Mg- 5.25wt.%Zn-0.6wt.%Ca alloy as biodegradable metal. *Sci. China Mater.* 61, 619–628. doi: 10.1007/s40843-017-9205-x

Gu, X., Zheng, Y., Cheng, Y., Zhong, S., and Xi, T. (2009). *In vitro* corrosion and biocompatibility of binary magnesium alloys. *Biomaterials* 30, 484–498. doi: 10.1016/j.biomaterials.2008.10.021

Haghshenas, M. (2017). Mechanical characteristics of biodegradable magnesium matrix composites: a review. *J. Magnes. Alloys* 5, 189–201. doi: 10.1016/j.jma.2017.05.001

He, G., Wu, Y., Zhang, Y., Zhu, Y., Liu, Y., Li, N., et al. (2015). Addition of Zn to the ternary Mg–Ca–Sr alloys significantly improves their antibacterial properties. *J. Mater. Chem. B* 3, 6676–6689. doi: 10.1039/C5TB01319D

He, J., Liu, T., Xu, S., and Zhang, Y. (2013). The effects of compressive pre-deformation on yield asymmetry in hot-extruded Mg−3Al−1Zn alloy. *Mater. Sci. Eng. A* 579, 1–8. doi: 10.1016/j.msea.2013.04.115

Hernandez-Rodriguez, M. A. L., Mercado-Solis, R. D., Presbítero, G., Lozano, D. E., Martinez-Cazares, G. M., and Bedolla-Gil, Y. (2019). Influence of boron additions and heat treatments on the fatigue resistance of CoCrMo alloys. *Materials* 12:1076. doi: 10.3390/ma12071076

Hou, L., Li, Z., Zhao, H., Pan, Y., Pavlinich, S., Liu, X., et al. (2016). Microstructure, mechanical properties, corrosion behavior and biocompatibility of as-extruded biodegradable Mg−3Sn−1Zn−0.5Mn Alloy. *J. Mater. Sci. Technol.* 32, 874–882. doi: 10.1016/j.jmst.2016.07.004

Jiang, W., Cipriano, A. F., Tian, Q., Zhang, C., Lopez, M., Sallee, A., et al. (2018). *In vitro* evaluation of MgSr and MgCaSr alloys via direct culture with bone marrow derived mesenchymal stem cells. *Acta Biomater.* 72, 407–423. doi: 10.1016/j.actbio.2018.03.049

Jiang, W., Wang, J., Zhao, W., Liu, Q., Jiang, D., and Guo, S. (2019). Effect of Sn addition on the mechanical properties and bio-corrosion behavior of cytocompatible Mg−4Zn based alloys. *J. Magnes. Alloys* 7, 15–26. doi: 10.1016/j.jma.2019.02.002

Kaur, M., and Singh, K. (2019). Review on titanium and titanium based alloys as biomaterials for orthopaedic applications. *Mater. Sci.Eng. C* 102, 844–862. doi: 10.1016/j.msec.2019.04.064

Koltygin, A., Bazhenov, V., and Mahmadiyorov, U. (2017). Influence of Al−5Ti−1B master alloy addition on the grain size of AZ91 alloy. *J. Magnes. Alloys* 5, 313–319. doi: 10.1016/j.jma.2017.08.002

Kubásek, J., Vojtěch, D., Lipov, J., and Ruml, T. (2013). Structure, mechanical properties, corrosion behavior and cytotoxicity of biodegradable Mg–X (X=Sn, Ga, In) alloys. *Mater. Sci. Eng. C* 33, 2421–2432. doi: 10.1016/j.msec.2013.02.005

Li, L. Y., Cui, L. Y., Zeng, R. C., Li, S. Q., Chen, X. B., Zheng, Y. F., et al. (2018). Advances in functionalized polymer coatings on biodegradable magnesium alloys – a review. *Acta Biomater.* 79, 23–36. doi: 10.1016/j.actbio.2018.08.030

Li, M., He, P., Wu, Y., Zhang, Y., Xia, H., Zheng, Y., et al. (2016). Stimulatory effects of the degradation products from Mg-Ca-Sr alloy on the osteogenesis through regulating ERK signaling pathway. *Sci. Rep.* 6:32323. doi: 10.1038/srep32323

Li, P., Zhang, H., Tong, T., and He, Z. (2019). The rapidly solidified β-type Ti–Fe–Sn alloys with high specific strength and low elastic modulus. *J. Alloys Compd.* 786, 986–994. doi: 10.1016/j.jallcom.2019.01.346

Liao, H., Kim, J., Liu, T., Tang, A., She, J., Peng, P., et al. (2019). Effects of Mn addition on the microstructures, mechanical properties and work-hardening of Mg-1Sn alloy. *Mater. Sci. Eng. A* 754, 778–785. doi: 10.1016/j.msea.2019.02.021

Liu, P., Wang, J. M., Yu, X. T., Chen, X. B., Li, S. Q., Chen, D. C., et al. (2019). Corrosion resistance of bioinspired DNA-induced Ca–P coating on biodegradable magnesium alloy. *J. Magnes. Alloys* 7, 144–154. doi: 10.1016/j.jma.2019.01.004

Liu, Y., Wu, Y., Bian, D., Gao, S., Leeflang, S., Guo, H., et al. (2017). Study on the Mg-Li-Zn ternary alloy system with improved mechanical properties, good degradation performance and different responses to cells. *Acta Biomater.* 62, 418–433. doi: 10.1016/j.actbio.2017.08.021

Liu, Y., Zheng, Y., Chen, X. H., Yang, J. A., Pan, H., Chen, D., et al. (2019). Fundamental theory of biodegradable metals—definition, criteria, and design. *Adv. Funct. Mater.* 29:1805402. doi: 10.1002/adfm.201805402

Lv, Y., Ding, Z., Xue, J., Sha, G., Lu, E., Wang, L., et al. (2018). Deformation mechanisms in surface nano-crystallization of low elastic modulus Ti6Al4V/Zn composite during severe plastic deformation. *Scr. Mater.* 157, 142–147. doi: 10.1016/j.scriptamat.2018.08.007

Majumdar, T., Eisenstein, N., Frith, J. E., Cox, S. C., and Birbilis, N. (2018). Additive manufacturing of titanium alloys for orthopedic applications: A materials science viewpoint. *Adv. Eng. Mater.* 20:1800172. doi: 10.1002/adem.201800172

Mehjabeen, A., Song, T., Xu, W., Tang, H. P., and Qian, M. (2018). Zirconium alloys for orthopaedic and dental applications. *Adv. Eng. Mater.* 20:1800207. doi: 10.1002/adem.201800207

Nie, J. F. (2003). Effects of precipitate shape and orientation on dispersion strengthening in magnesium alloys. *Scr. Mater.* 48, 1009–1015. doi: 10.1016/S1359-6462(02)00497-9

Nie, J. F. (2012). Precipitation and hardening in magnesium alloys. *Metall. Mater. Trans. A* 43, 3891–3939. doi: 10.1007/s11661-012-1217-2

Noronha Oliveira, M., Schunemann, W. V. H., Mathew, M. T., Henriques, B., Magini, R. S., Teughels, W., et al. (2018). Can degradation products released from dental implants affect peri-implant tissues? *J. Periodontal Res.* 53, 1–11. doi: 10.1111/jre.12479

Pan, F., Xu, A., Deng, D., Ye, J., Jiang, X., Tang, A., et al. (2016). Effects of friction stir welding on microstructure and mechanical properties of magnesium alloy Mg-5Al-3Sn. *Mater. Des.* 110, 266–274. doi: 10.1016/j.matdes.2016.07.146

Pan, H., Fu, H., Ren, Y., Huang, Q., Gao, Z., She, J., et al. (2016). Effect of Cu/Zn on microstructure and mechanical properties of extruded Mg–Sn alloys. *Mater. Sci. Technol.* 32, 1240–1248. doi: 10.1080/02670836.2015.1115604

Pan, H., Qin, G., Huang, Y., Ren, Y., Sha, X., Han, X., et al. (2018). Development of low-alloyed and rare-earth-free magnesium alloys having ultra-high strength. *Acta Mater.* 149, 350–363. doi: 10.1016/j.actamat.2018.03.002

Pan, H., Qin, G., Xu, M., Fu, H., Ren, Y., Pan, F., et al. (2015). Enhancing mechanical properties of Mg–Sn alloys by combining addition of Ca and Zn. *Mater. Des.* 83, 736–744. doi: 10.1016/j.matdes.2015.06.032

Peng, P., He, X., She, J., Tang, A., Rashad, M., Zhou, S., et al. (2019). Novel low-cost magnesium alloys with high yield strength and plasticity. *Mater. Sci. Eng. A* 766:138332. doi: 10.1016/j.msea.2019.138332

Peng, P., Tang, A., Chen, X., She, J., Zhou, S., Song, J., et al. (2018). Microstructure and mechanical properties of Mg−6Al−1Sn−0.3Mn alloy sheet fabricated through extrusion combined with rolling. *Crystals* 8:356. doi: 10.3390/cryst8090356

Radha, R., and Sreekanth, D. (2017). Insight of magnesium alloys and composites for orthopedic implant applications – a review. *J. Magnes. Alloys* 5, 286–312. doi: 10.1016/j.jma.2017.08.003

Salleh, E. M., Zuhailawati, H., and Ramakrishnan, S. (2018). Synthesis of biodegradable Mg-Zn alloy by mechanical alloying: statistical prediction of elastic modulus and mass loss using fractional factorial design. *T. Nonferr. Metal. Soc.* 28, 687–699. doi: 10.1016/S1003-6326(18)64701-6

Schaller, B., Saulacic, N., Beck, S., Imwinkelried, T., Goh, B. T., Nakahara, K., et al. (2016). In vivo degradation of a new concept of magnesium-based rivet-screws in the minipig mandibular bone. *Mater. Sci. Eng. C* 69, 247–254. doi: 10.1016/j.msec.2016.06.085

She, J., Pan, F., Hu, H., Pan, H., Tang, A., Song, K., et al. (2015). Microstructures and mechanical properties of as-extruded Mg−5Sn−1Zn–xAl (x=1, 3 and 5) alloys. *Prog. Nat. Sci. Mater.* 25, 267–275. doi: 10.1016/j.pnsc.2015.08.007

She, J., Pan, F., Zhang, J., Tang, A., Luo, S., Yu, Z., et al. (2016). Microstructure and mechanical properties of Mg–Al–Sn extruded alloys. *J. Alloys Compd.* 657, 893–905. doi: 10.1016/j.jallcom.2015.10.146

Song, B., Ruiz-Trejo, E., and Brandon, N. P. (2018). Enhanced mechanical stability of Ni-YSZ scaffold demonstrated by nanoindentation and electrochemical impedance spectroscopy. *J. Power Sources* 395, 205–211. doi: 10.1016/j.jpowsour.2018.05.075

Song, B., She, J., Guo, N., Qiu, R., Pan, H., Chai, L., et al. (2019). Regulating precipitates by simple cold deformations to strengthen Mg alloys: a review. *Materials* 12:2507. doi: 10.3390/ma12162507

Takale, A. M., and Chougule, N. K. (2019). Effect of wire electro discharge machining process parameters on surface integrity of Ti49.4Ni50.6 shape memory alloy for orthopedic implant application. *Mater. Sci. Eng. C* 97, 264–274. doi: 10.1016/j.msec.2018.12.029

Tong, T., Zhang, F., Liu, S., Du, Y., and Li, K. (2017). Experimental investigation on the phase equilibria of the Mg-Sn-Ag system in the Mg-rich corner. *J. Magnes. Alloys* 5, 41–47. doi: 10.1016/j.jma.2017.02.003

Wang, B. J., Luan, J. Y., Xu, D. K., Sun, J., Li, C. Q., and Han, E. H. (2019a). Research progress on the corrosion behavior of magnesium-lithium-based alloys: a review. *Acta. Metall. Sin.* 32, 1–9. doi: 10.1007/s40195-018-0847-9

Wang, B. J., Xu, D. K., Sheng, L. Y., Han, E. H., and Sun, J. (2019b). Understanding to the deformation and fracture mechanisms of an annealing-tailored "bimodal" grain-structured Mg alloy. *J. Mater. Sci. Technol.* 35, 2423–2429. doi: 10.1016/j.jmst.2019.06.008

Wang, B. J., Xu, D. K., Sun, J., and Han, E. H. (2019c). Effect of grain structure on the stress corrosion cracking (SCC) behavior of an as-extruded Mg-Zn-Zr alloy. *Corros. Sci.* 157, 347–356. doi: 10.1016/j.corsci.2019.06.017

Wang, B. J., Xu, D. K., Wang, S. D., and Han, E. H. (2019d). Recent progress in the research about fatigue crack initiation of Mg alloys under elastic stress amplitudes: a review. *Front. Mech. Eng.* 14, 113–127. doi: 10.1007/s11465-018-0482-1

Wang, B. J., Xu, D. K., Wang, S. D., Sheng, L. Y., Zeng, R. C., and Han, E. H. (2019e). Influence of solution treatment on the corrosion fatigue behavior of an as-forged Mg-Zn-Y-Zr alloy. *Int. J. Fatigue* 120, 46–55. doi: 10.1016/j.ijfatigue.2018.10.019

Wang, P., Guo, E., Wang, X., Kang, H., Chen, Z., Cao, Z., et al. (2019f). The influence of Sc addition on microstructure and tensile mechanical properties of Mg−4.5Sn−5Zn alloys. *J. Magnes. Alloys* 7, 456–465. doi: 10.1016/j.jma.2019.05.004

Yamamoto, A., Honma, R., and Sumita, M. (1998). Cytotoxicity evaluation of 43 metal salts using murine fibroblasts and osteoblastic cells. *J. Biomed. Mater. Res.* 39, 331–340. doi: 10.1002/(sici)1097-4636(199802)39:2<331::aid-jbm22>3.0.co;2-e

Yu, H., Sun, Y., Hu, L., Wan, Z., and Zhou, H. (2017). The effect of Ti addition on microstructure evolution of AZ61 Mg alloy during mechanical milling. *J. Alloys Compd.* 704, 537–544. doi: 10.1016/j.jallcom.2017.02.029

Yu, H., Xin, Y., Wang, M., and Liu, Q. (2018). Hall-Petch relationship in Mg alloys: a review. *J. Mater. Sci. Technol.* 34, 248–256. doi: 10.1016/j.jmst.2017.07.022

Yu, Z., Tang, A., He, J., Gao, Z., She, J., Liu, J., et al. (2018). Effect of high content of manganese on microstructure, texture and mechanical properties of magnesium alloy. *Mater. Charact.* 136, 310–317. doi: 10.1016/j.matchar.2017.12.029

Yu, Z., Tang, A., Wang, Q., Gao, Z., He, J., She, J., et al. (2015). High strength and superior ductility of an ultra-fine grained magnesium–manganese alloy. *Mater. Sci. Eng. A* 648, 202–207. doi: 10.1016/j.msea.2015.09.065

Yu, Z., Tang, A., Zhang, L., and Pan, F. (2014). Effect of microalloying with titanium on microstructure and mechanical properties of AZ91 magnesium alloy. *Mater. Sci. Technol.* 30, 1441–1446. doi: 10.1179/1743284714Y.0000000528

Zhang, J. L., Zheng, Y. Q., and Wang, Z. M. (2015). Effects of Ti on microstructure and properties of as-extruded Mg-10Al-2Zn alloy after heat treatment. *Heat Treat. Metals.* 40, 30–34. doi: 10.13251/j.issn.0254-6051.2015.08.005

Zhang, M., Zhang, W. Z., and Zhu, G. Z. (2008). The morphology and crystallography of polygonal Mg_2Sn precipitates in a Mg–Sn–Mn–Si alloy. *Scr. Mater.* 59, 866–869. doi: 10.1016/j.scriptamat.2008.06.033

Zhao, D., Witte, F., Lu, F., Wang, J., Li, J., and Qin, L. (2017). Current status on clinical applications of magnesium-based orthopaedic implants: a review from clinical translational perspective. *Biomaterials* 112, 287–302. doi: 10.1016/j.biomaterials.2016.10.017

Zhen, Z., Xi, T., Zheng, Y., Li, L., and Li, L. (2014). *In vitro* study on Mg–Sn–Mn alloy as biodegradable metals. *J. Mater. Sci. Technol.* 30, 675–685. doi: 10.1016/j.jmst.2014.04.005

Conflict of Interest: The authors declare that the research was conducted in the absence of any commercial or financial relationships that could be construed as a potential conflict of interest.

Copyright © 2020 Yu, Zhang, Tang, Li, Liu, Gao and Pan. This is an open-access article distributed under the terms of the Creative Commons Attribution License (CC BY). The use, distribution or reproduction in other forums is permitted, provided the original author(s) and the copyright owner(s) are credited and that the original publication in this journal is cited, in accordance with accepted academic practice. No use, distribution or reproduction is permitted which does not comply with these terms.